FEBS Letters 561 (2004) 22–28

FEBS 28086

AtHMA3, a plant P_{1B}-ATPase, functions as a Cd/Pb transporter in yeast

Antoine Gravot[1], Aurélie Lieutaud[1], Frédéric Verret, Pascaline Auroy, Alain Vavasseur, Pierre Richaud*

CEA Cadarache, DSV/DEVM/Laboratoire des Echanges Membranaires et Signalisation, UMR 6191 CNRS-CEA-Aix-Marseille II, Bat. 156, 13108 St Paul lez Durance Cedex, France

Received 17 December 2003; revised 15 January 2004; accepted 15 January 2004

First published online 16 February 2004

Edited by Ulf-Ingo Flügge

Abstract **The *Arabidopsis thaliana* AtHMA3 protein belongs to the P_{1B}-adenosine triphosphatase (ATPase) transporter family, involved in heavy metal transport. Functional expression of AtHMA3 phenotypically complements the Cd/Pb-hypersensitive yeast strain Δ*ycf1*, but not the Zn-hypersensitive mutant Δ*zrc1*. AtHMA3-complemented Δ*ycf1* cells accumulate the same amount of cadmium as YCF1-complemented Δ*ycf1* cells or wild-type cells, suggesting that AtHMA3 carries out an intracellular sequestration of Cd. A mutant of AtHMA3 altered in the P-ATPase phosphorylation domain did not complement Δ*ycf1*, suggesting that metal transport rather than chelation is involved. The fusion protein AtHMA3::green fluorescent protein (GFP) is localized at the vacuole, consistent with a role in the influx of cadmium into the vacuolar compartment. In *A. thaliana*, the mRNA of AtHMA3 was detected mainly in roots, old rosette leaves and cauline leaves. The expression levels were not affected by cadmium or zinc treatments.**

Key words: P-type adenosine triphosphatase; AtHMA3; Cadmium; Lead; Zinc; Metal tolerance; *Arabidopsis*

1. Introduction

P-adenosine triphosphatases (ATPases) are ubiquitous intramembranous proteins involved in the transport of various compounds including protons, ions and phospholipids. This type transporter differs from other ATPase families in that phosphorylation of a conserved Asp is a key step involved in their catalytic cycle [1,2]. The *Arabidopsis thaliana* genome exhibits not less than eight genes coding for P_{1B}-ATPases, a subgroup implicated in heavy metal transport [3]. Heavy metal transporters are involved in oligoelement acquisition and compartmentation but also in toxic heavy metal absorption and detoxification. Heavy metal accumulation in crops is a major problem in agriculture and human health. Conversely, accumulation of metal by plants is used in a soil depollution technique called phytoremediation. Understanding of these phenomena at the molecular level is broadly recognized as a priority, as it can lead to the development of genetically modified crops which could meet technical needs [4–6].

From the eight members of the *Arabidopsis* P_{1B}-ATPases recently renamed AtHMA1–AtHMA8 [3], it was demonstrated that at least two of them are involved in copper trafficking in planta: RAN1/AtHMA7 [7,8] and PAA1/AtHMA6 [9]. RAN1 is involved in delivering Cu to an ethylene receptor, and PAA1 is involved in Cu import in the chloroplast for further integration in two cuproproteins of major importance: the Cu/Zn superoxide dismutase (Cu/Zn SOD) and the thylakoid lumen protein plastocyanine. These data suggest that plant heavy metal P-ATPases are involved in homeostasis and compartmentation of metals that are essential for the plant metabolism, although they are potentially highly toxic if present at excessive concentrations in cells.

Sequence alignments show that AtHMA1–4 exhibit high similarity with Zn/Cd/Pb/Co ATPases previously characterized in prokaryotes [10]. In microorganisms, proteins of this subgroup participate in cell detoxification [11]. Their expression levels are regulated by the metal environmental status, revealing an integrated detoxification process [12–14]. In *Arabidopsis*, AtHMA2, AtHMA3 and AtHMA4 exhibit the most closely related sequences, differing mainly in the length of the C-terminal part. *AtHMA4* gene is located on chromosome 2 whereas *AtHMA2* and *AtHMA3* are present in tandem on chromosome 4. A recent work demonstrates that heterologous expression of *AtHMA4* enhances Cd tolerance in yeast and complements a zinc-hypersensitive mutant strain of *Escherichia coli*. The results suggest that AtHMA4 could transport zinc and cadmium [15]. However, the exact physiological function of these proteins in planta is still unclear. Do they participate in the absorption and/or trafficking of zinc – an essential nutrient – into plant organs? Conversely do they help the plant to avoid toxic metal absorption at the root level, or contribute to their sequestration in specialized organs (trichomes) or organelles (vacuoles)?

To answer those questions, it is first necessary to characterize the metal transport activity of these proteins. The present work reports the cloning, heterologous expression in yeast and functional characterization of AtHMA3. We also analyzed the mRNA expression and a possible regulation of the transcript levels in planta.

2. Materials and methods

2.1. Yeast strains, media

The BY4741 wild-type *Saccharomyces cerevisiae* strain (EUROSCARF acc. no. Y00000), the cadmium-sensitive Δ*ycf1* (Y04069)

*Corresponding author. Fax: (33)-4 42 25 23 64.
E-mail address: pierre.richaud@cea.fr (P. Richaud).

[1] Equal contribution of these authors.

Abbreviations: GFP, green fluorescent protein; Ws, Wassilewskija; Col, Columbia

0014-5793/04/$30.00
doi:10.1016/S0014-5793(04)00072-9

strain and the zinc-sensitive strain Δ*zrc1* (Y00829) were used for AtHMA3 heterologous expression and phenotype characterization. Synthetic yeast medium without uracil (S-URA) (yeast nitrogen base (Sigma) 6.7 g l^{-1}, drop out (Sigma) 1.92 g l^{-1}) was used with additional 2% (w/v) raffinose for yeast precultures, and with 2% (w/v) galactose and 1% (w/v) raffinose for induction during metal tolerance experiments on solid medium. Alternatively, liquid medium inductions were conducted using 2% (w/v) galactose as unique source of carbon.

2.2. Cloning of the HMA3 cDNA

Total RNA was extracted from leaves of *A. thaliana* (Wassilewskija (Ws) ecotype) according to [16]. *AtHMA3* full-length cDNA was amplified through reverse transcription-polymerase chain reaction (RT-PCR) using the Omniscript reverse transcriptase (Invitrogen™) and the expand high fidelity Taq polymerase (Roche Diagnostics). RT was performed using 4 μg of total RNA and an oligo$(dT)_{20}$ primer. cDNA was amplified using the following oligonucleotides: 5′-HMA3 (5′-CAAGCTCAACGATGGCGGAAGGTG-3′) and 3′-HMA3 (5′-CAGAAGAAGGTTTTCACTTTTG-3′), designed on the Columbia (Col) genomic sequence At4g30120 in order to amplify the *AtHMA3* open reading frame (ORF).

The complete cDNA sequence was subcloned in the pCR®-XL-TOPO vector (Invitrogen™) and was sequenced using a Perkin Elmer ABI Prism 310 sequencer. *AtHMA3* was then cloned into the *Not*I site of the yeast expression vector pYES2 (Invitrogen™) downstream the pGAL promoter, resulting in plasmid pRP310. A pYES2-green fluorescent protein (GFP) plasmid was constructed by introducing the *Eco*RI/*Not*I fragment from the pEGFP-N2 vector (Clontech) into the *Eco*RI/*Not*I sites of pYES2. *AtHMA3* was then cloned in frame with the *EGFP* gene into the *Spe*I and *Pst*I sites of the pYES2-GFP vector, resulting in plasmid pLA312, allowing the yeast expression of a AtHMA3::GFP fusion protein. The pAG314 plasmid was generated with the Quickchange site-directed mutagenesis kit from Stratagene, using the plasmid pRP310 as template and the H3D397A forward and H3D397A reverse couple of primers (Table 1). The pAG314 plasmid codes for a D397A mutant of AtHMA3 which is unable to form the aspartyl-phosphate intermediate involved in the P-type ATPase catalytic cycle [2]. Another construction was performed in pYES2 containing a YCF1::GFP construction into the *Sac*I/*Not*I sites, allowing the complementation of the Δ*ycf1* strain. Yeast strains were transformed using the LiAc technique [17], using uracil complementation for selection.

2.3. Fluorescence microscopy

Yeast vacuolar membranes were stained with FM4-64 according to [18]. Yeast cells were observed through confocal microscopy (Fluoview Olympus, France) using a krypton/argon laser. Excitation for GFP and FM4-64 was performed at 488 nm, and recordings were performed at 510–550 nm for GFP and at 585–610 nm for FM4-64.

2.4. Metal tolerance experiments

Yeast inductions were performed at 30°C during 8 h with galactose-containing medium. Cultures were subsequently diluted to optical density $(OD)_{600} = 0.1$, and 2 μl were spotted on solid induction medium supplemented with $ZnSO_4$, $Pb(NO_3)_2$ or $CdCl_2$. Incubations were performed up to 5 days at 30°C. Alternatively, induced cultures were diluted to $OD_{600} = 0.2$ and grown in liquid medium at 30°C aerobically, and OD_{600} was followed at various times over 48 h. Generation times were calculated over the early exponential growth phase. Pb experiments were not conducted in liquid medium, as this metal is hardly soluble in the yeast culture medium.

2.5. Induced coupled plasma (ICP) experiments

Cells were first grown for 24 h in the induction medium described above, then for 48 h in 20 ml of 40 μM cadmium-containing induction medium. After centrifugation, supernatants were collected, cells were washed three times with ethylenediamine tetraacetic acid (EDTA) 10 mM, pelleted, dried for 48 h at 50°C and mineralized. The cadmium content was determined both in the medium and cells, using ICP (ICP OES Vista MPX, Varian).

2.6. mRNA expression levels in Arabidopsis

A. thaliana (ecotype Col-0) plants were hydroponically grown from 1 h to 7 days with various concentrations of $CdCl_2$ (0–50 μM) and $ZnSO_4$ (3–500 μM). The nutritive solution was as follows: $Ca(NO_3)_2$ 0.8 mM; KNO_3 2 mM; K_2HPO_4 60 μM; KH_2PO_4 695 μM; $MgSO_4$ 1.1 mM; $FeSO_4$ 20 μM; Na_2EDTA 20 μM; $(NH_4)_6Mo_7O_{24}$ 74 nM; $MnSO_4$ 3.6 μM; $ZnSO_4$ 3 μM; H_3BO_3 9.25 μM; $CuSO_4$ 785 nM. For tissular mRNA distribution, plants were grown on sand up to 2 months with a 8 h photoperiod, and tissues were collected and stored in liquid nitrogen before RNA extraction. Total RNA were extracted from various plant tissues with Trizol (Life Technologies). RT was performed using 4 μg total RNA using the reverse first strand cDNA synthesis kit (Amersham). PCRs were performed using ExTaq polymerase (TaKaRa) and cycles of 94°C for 30 s/55°C for 30 s/72°C for 30 s and the primers reported in Table 1. Actin was used as a control as described in [19]. PCR samples were taken at successive cycles and analyzed by agarose gel electrophoresis for quantification, checking that amplification did not reach saturation. Two independent experiments were conducted and gave similar results.

3. Results

3.1. Cloning of the HMA3 cDNA

The nucleic sequence of *AtHMA3* cDNA (ecotype Ws) was determined (GenBank AY055217) and compared to the published genomic sequence (ecotype Col, At4g30120). The intron/exon distribution in *AtHMA3* shows the same organization as those of *AtHMA4* and *AtHMA2* from *Arabidopsis*, as described previously [3]. Nevertheless, the two first introns are remarkably short in *AtHMA3* (around 200 bp), contrasting with the two large first introns of around 1–1.5 kb in *AtHMA4* and *AtHMA2*. Conceptual translation of the cDNA predicted a polypeptide of 760 amino acids with significant amino acid similarity with many P-ATPases involved in the Cd/Zn transport, including CadA from *Listeria monocytogenes*. The few divergences between Col and Ws *AtHMA3* sequences were controlled by various independent PCRs on genomic DNA and cDNA, with subsequent sequencing of the products. These ecotypic divergences (I vs. R in position 448; I vs. M in 699 and S vs. A in 714) are not located in the classical ATPase functional domains (Fig. 1). The N-terminal part of AtHMA3 exhibits only one degenerated HMA signature of 29–31 residues as defined by PROSITE (PS01047), with a replacement of the canonical motif GMxCxxC by GICCxxx. This modification is an unusual feature shared with AtHMA2, AtHMA3 and AtHMA4. The amino acid se-

Table 1
Primers used for mRNA level quantification by RT-PCR and for site-directed mutagenesis

Name	Sequence
Actin F	5′-GGCCGATGGTGAGGATATTCAGCCACTTG-3′
Actin R	5′-TCGATGGACCTGACTCATCGTACTCACTC-3′
HMA3 For	5′-GCTACTATGAAGCGAGG-3′
HMA3 Rev	5′-GGTAACATGTAGACACGG-3′
HMA4 For	5′-CCGGTGCAGATTATTGG-3′
HMA4 Rev	5′-TCTACCTTGACGGCTC-3′
H3D397A For	5′-GATCAAGATTGTTGCTTTTGCCAAAACAGGAACTATTACAAAGGC-3′
H3D397A Rev	5′-GCCTTTGTAATAGTTCCTGTTTTGGCAAAAGCAACAATCTTGATC-3′

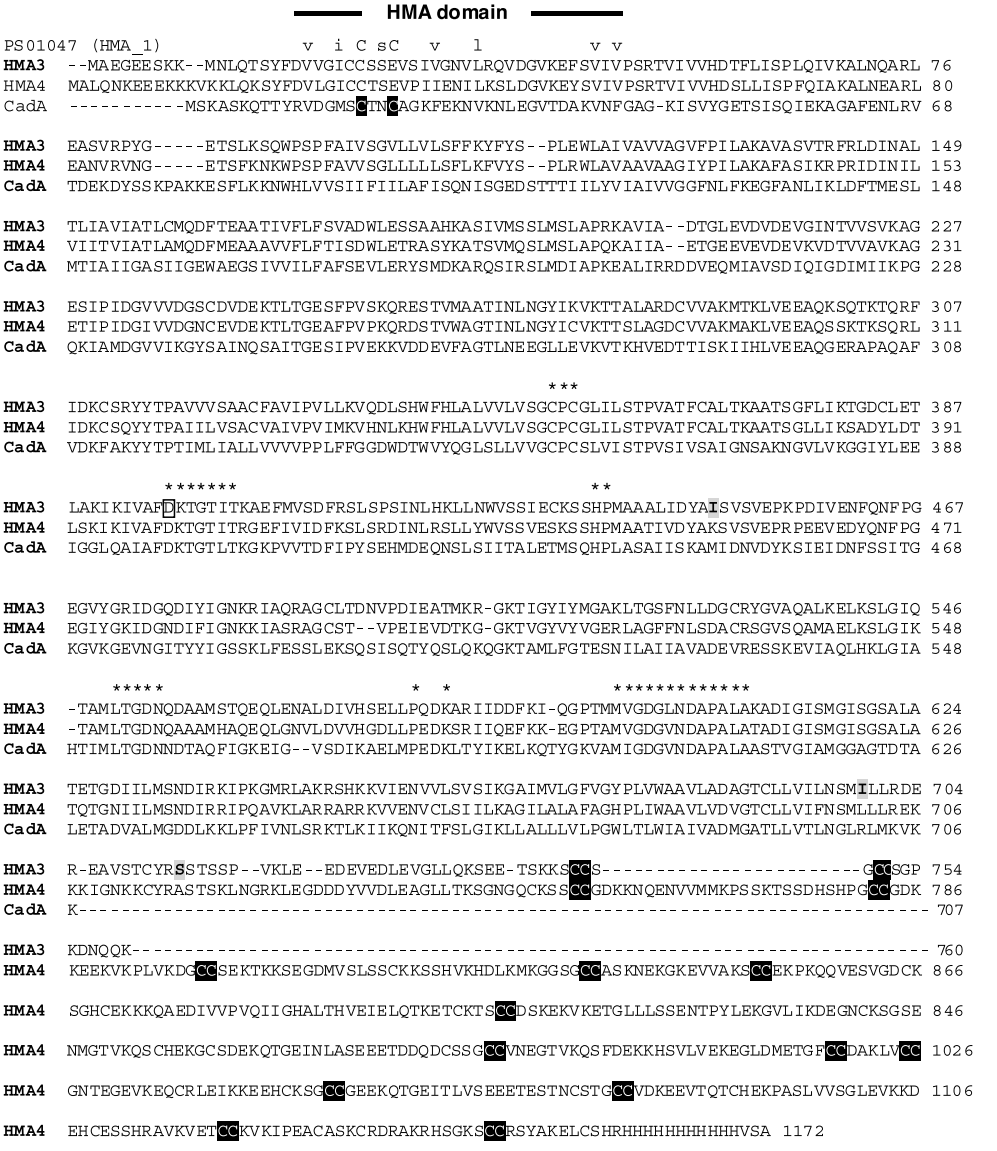

Fig. 1. Alignment of AtHMA3 (AAL16382) and AtHMA4 (AAL84162) from *A. thaliana* (Ws) and CadA (P58414) from *L. monocytogenes*, realized with Clustal W. The HMA_1 consensus as defined by PROSITE (PS01047), is represented. Cysteine residues of the classical HMA domain are highlighted in the CadA sequence. C-terminal cysteine pairs are highlighted in the AtHMA3 and AtHMA4 sequences. Ecotypic variations between Col and Ws sequences are highlighted. Classical P-ATPase consensus sequences as described in [26] are marked with a star (*). The D397 from the phosphorylation consensus site which was converted to alanine in the hma3-P(-) modified protein is boxed.

quence is also very similar to AtHMA4, another P-ATPase from *A. thaliana*, along the whole AtHMA3 length. Nevertheless, AtHMA3 does not present the long AtHMA4 C-terminal extension with numerous cysteine pairs and an 11 histidine stretch (Fig. 1), a very unusual feature among the P-ATPase family.

3.2. *HMA3 expression enhances Cd tolerance in a yeast Cd-sensitive strain*

3.2.1. Solid medium experiments. In our experimental conditions, the wild-type yeast strain was able to grow up to 80–90 μM of $CdCl_2$. Beyond this range, the growth rate was drastically reduced and stopped for Cd concentrations above 150 μM. A Cd-sensitive mutant strain, deleted for the *ycf1* gene as reported by [20], was also used to minimize redundant Cd detoxification processes. In the present study, the Δ*ycf1* strain exhibits a severe growth reduction for $CdCl_2$ concentrations above 70 μM. As shown in Fig. 2, heterologous expression of AtHMA3 in the wild-type strain did not enhance yeast resistance to Cd. The expression of AtHMA3 fully complements the Δ*ycf1* strain up to 70 μM of $CdCl_2$. For latter concentrations (90–150 μM), the complementation was only partial, compared to Δ*ycf1*-YCF1. Fig. 2 also shows that AtHMA3::GFP transformed in Δ*ycf1* induced a less efficient complementation than AtHMA3.

It was recently demonstrated that the Δ*ycf1* strain is sensitive to lead [6]. We used this strain to test a possible Pb tolerance enhancement by AtHMA3. As shown in Fig. 3, AtHMA3 complemented the Pb hypersensitivity of Δ*ycf1* for concentrations around 50 mM. However, AtHMA3 expression did not enhance wild-type yeast resistance to Pb. It is noticeable that the fusion AtHMA3::GFP did not complement Δ*ycf1* concerning the tolerance to lead.

Finally, similar experiments were conducted to test the abil-

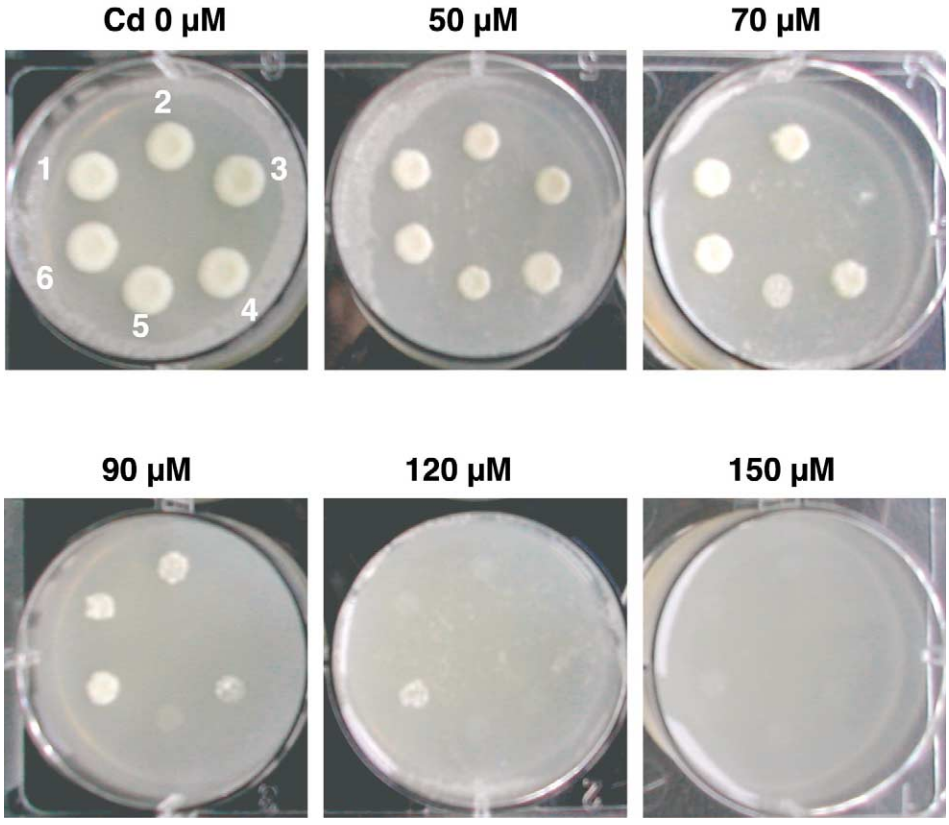

Fig. 2. Growth of wild-type yeast and Δ*ycf1* (Cd/Pb-hypersensitive mutant) cells transformed with empty vector pYES2 (control) or with the plasmids pRP310 (AtHMA3) and pLA312 (AtHMA3::GFP), in the presence of various cadmium concentrations. (1) WT-pYES2; (2) WT-AtHMA3; (3) Δ*ycf*1-pYES2; (4) Δ*ycf1*-AtHMA3; (5) Δ*ycf1*-AtHMA3::GFP; (6) Δ*ycf1*-YCF1.

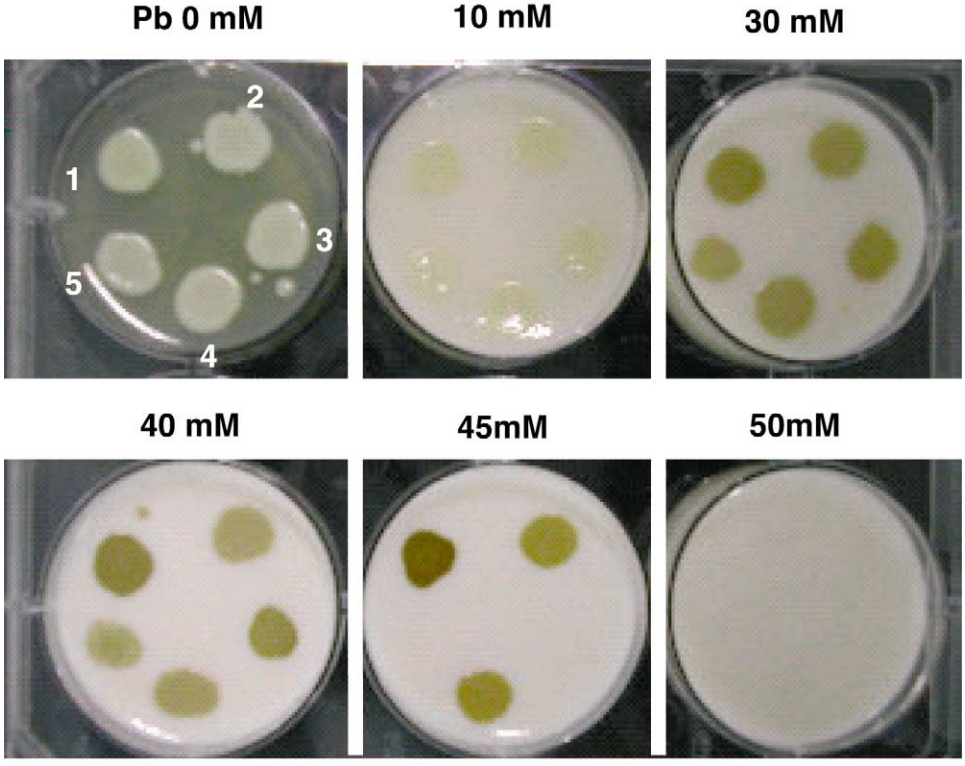

Fig. 3. Growth of yeast strains in the presence of various lead concentrations. (1) WT-pYES2; (2) WT-AtHMA3; (3) Δ*ycf1*-pYES2; (4) Δ*ycf1*-AtHMA3; (5) Δ*ycf1*-AtHMA3::GFP.

Table 2
Generation times measured during early exponential growth phase with or without 40 μM cadmium, on synthetic medium without uracil and galactose 2% as unique carbon source

	Generation time (h)	
	Cd (0 μM)	Cd (40 μM)
WT	2.28 (±0.01)	4.46 (±0.01)
WT+AtHMA3	2.33 (±0.15)	4.73 (±0.58)
Δ*ycf1*	2.27 (±0.07)	7.07 (±0.22)
Δ*ycf1*+AtHMA3	2.25 (±0.04)	5.20 (±0.06)
Δ*ycf1*+AtHMA3::GFP	2.35 (±0.05)	5.67 (±0.36)
Δ*ycf1*+YCF1	2.28 (±0.15)	4.29 (±0.16)
Δ*ycf1*+AtHMA3-D397A	2.38 (±0.16)	6.97 (±0.44)

Values are means of duplicate experiments.

ity of AtHMA3 to enhance Zn tolerance in the yeast wild-type and in the zinc-sensitive mutant Δ*zrc1*. We found that yeast tolerance to Zn was not affected by the expression of AtHMA3, even in the Zn-sensitive mutant (data not shown).

3.2.2. Liquid medium experiments. All strains that we used exhibited very similar generation times when grown without metal. In the presence of 40 μM cadmium, the generation times were increased depending on the plasmid and were consistent with solid medium experiments, i.e. AtHMA3 complements Δ*ycf1* and the fusion protein AtHMA3::GFP partially complements Δ*ycf1* (Table 2). The exponential growth phase was very short for the Δ*ycf1* strain when exposed to Cd. As a consequence, differences between strains are more pronounced when considering the OD_{600} at 48 h data, i.e. at the stationary phase (Table 3).

To test whether Δ*ycf1* phenotypic complementation is due to transport or solely to a chelation phenomenon, we used a D397A mutant of AtHMA3 that we generated. Asp-397 is predicted to be the invariant residue that is the AtHMA3 phosphorylation site (boxed in the Fig. 1). The transport function of this mutant is therefore expected to be affected. Indeed, this mutant did not complement the Δ*ycf1* strain phenotype, suggesting that metal detoxification is grounded on AtHMA3 transport function. Semiquantitative RT-PCRs were conducted (using yeast actin mRNA as control) to verify that the mRNA transcript levels were identical in strains expressing AtHMA3 or the D397A mutant (data not shown).

3.3. Cd tolerance enhancement is not due to Cd expulsion into the culture medium

Following yeast culture in cadmium-containing medium (40 μM), Cd contents were determined in yeast pellets by ICP measurements (Table 4). AtHMA3 expression in wild-type did not change Cd sensitivity compared with the control (WT-pYES2) and it was not surprising to find that Cd accumulation was very similar in both strains. Nevertheless, when Δ*ycf1* was complemented by YCF1 or AtHMA3, Cd accumulations were also very similar to those obtained in the wild-type. These results suggest that AtHMA3 does not induce Cd release into the medium, but rather participates in the intracellular sequestering of the metal. YCF1 is indeed a transporter located in the vacuolar membrane, expulsing glutathione S-conjugated xenobiotics, including cadmium, to the vacuolar compartment.

Table 3
OD_{600} measured after a 48 h culture in presence or absence of 40 μM Cd, on synthetic medium without uracil and galactose 2% as unique carbon source

	OD_{600} at 48 h		% control
	Cd (0 μM)	Cd (40 μM)	
WT	12.9 (±0.6)	9.0 (±0.1)	69.7 (±2.4)
WT+AtHMA3	12.9 (±0.2)	7.8 (±0.1)	60.3 (±1.1)
Δ*ycf1*	13.4 (±0.1)	2.4 (±0.1)	17.7 (±1.0)
Δ*ycf1*+AtHMA3	13.9 (±1.1)	7.0 (±0.3)	50.2 (±1.7)
Δ*ycf1*+AtHMA3::GFP	12.9 (±0.6)	4.4 (±0.1)	34.3 (±2.2)
Δ*ycf1*+YCF1	12.7 (±0.6)	8.0 (±0.1)	63.2 (±3.4)
Δ*ycf1*+AtHMA3-D397A	13.9 (±0.7)	2.4 (±0.3)	16.1 (±0.7)

Values are means of triplicate experiments.

Table 4
Cadmium content found in cell pellets following 48 h exposition to 40 μM $CdCl_2$

	μg Cd per mg dry pellet	S.D.
WT-pYES2	0.27	0.02
WT-AtHMA3	0.31	0.02
Δ*ycf1*-YCF1	0.33	0.01
Δ*ycf1*-AtHMA3	0.30	0.01

Values are means of duplicate experiments.

3.4. HMA3::GFP localization experiments

FM4-64 was used as a control to visualize vacuolar membranes in yeast (Fig. 4). The GFP fluorescence was found to be very low, and was not found in all cells. Nevertheless, when present, it was always found inside vacuoles and colocalized with FM4-64 fluorescence, suggesting a vacuolar localization.

3.5. HMA3 tissular expression and metal-induced regulation in planta

Due to the high homology of *AtHMA2*, *AtHMA3* and *AtHMA4* cDNA sequences, primers were carefully designed in specific regions. Absence of cross-amplification was verified by PCR using plasmids containing *AtHMA2*, *AtHMA3* and *AtHMA4* as a matrix (data not shown). The *AtHMA3* expression level was not modulated when plants were treated with Zn (100–500 μM) or Cd (30 μM) in hydroponic conditions, for a few hours to one week (data not shown). AtHMA3 mRNA was detected in all plant parts but at weak levels, since at least 30 cycles of PCR were needed (Fig. 5). In the same conditions AtHMA4 was detected as soon as the 24th cycle. Highest levels of AtHMA3 mRNA were found in old rosette leaves, in roots and in cauline leaves.

4. Discussion

4.1. Evidences support the hypothesis of a AtHMA3-mediated Cd and Pb transport and intracellular sequestration in yeast

AtHMA3 is a P_{1B}-ATPase predicted to transport Zn, Cd, Pb and Co. The *S. cerevisiae* BY4741 strain exhibits only two P_{1B}-ATPases: CCC2 which is involved in providing copper to the extracytosolic domain of FET-3, an iron transporter [21], and PCA1 which is a putative copper transporter [22]. This wild-type strain does not contain CAD2, a PCA1 variant, which confers Cd resistance to the X3382-3A strain [23]. The major Cd resistance factor in BY4741 consists in the vacuolar glutathione S-conjugated pump YCF1, which belongs to the ABC superfamily and which mediates transport of Cd-GSH complex into the vacuole. It was recently demonstrated that YCF1 mediates also Pb vacuolar sequestration [6].

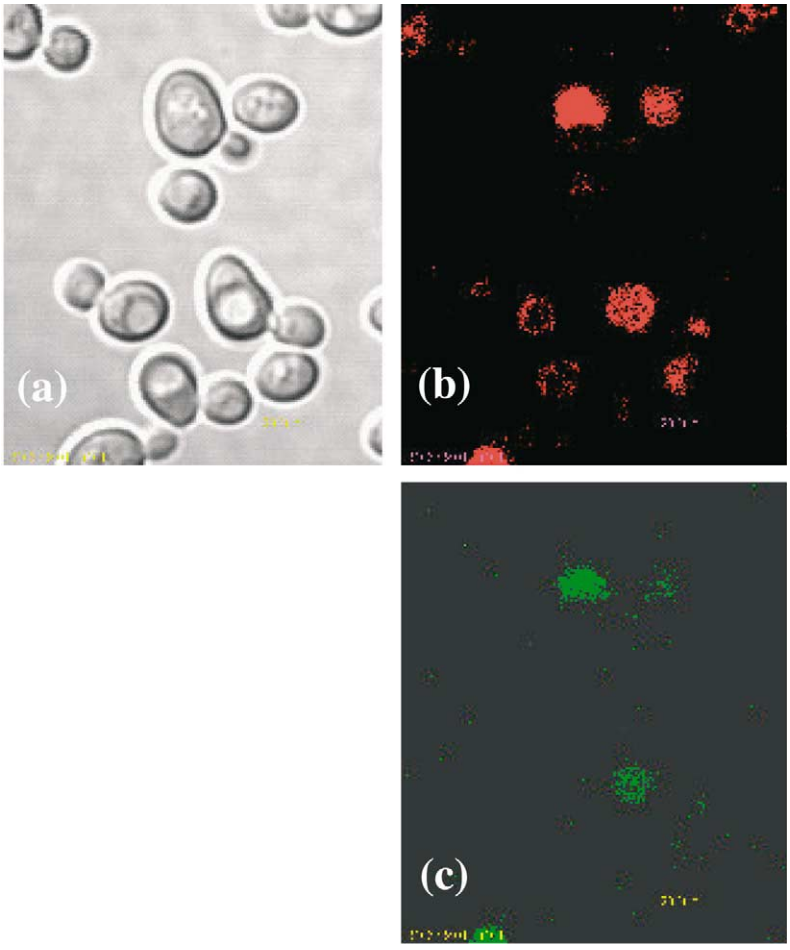

Fig. 4. AtHMA3::GFP fusion protein subcellular localization. Confocal microscope observations were performed following a 24 h induction. a; Transmission. b: FM4-64 fluorescence (excitation at 488 nm, emission between 585 and 610 nm). c: GFP fluorescence (excitation at 488 nm, emission measured between 510 and 550 nm).

Heterologous expression in yeast shows that AtHMA3 expression complements the Cd- and Pb-hypersensitive mutant Δ*ycf1*, suggesting a role of this protein in the detoxification of Cd and Pb. In the D397A mutant, the Asp-397 of the phosphorylation consensus domain is replaced by an Ala. This mutant is believed to be inactive in the transport function [2]. Our results show that AtHMA3-D397A does not complement at all the Δ*ycf1* mutant strain. This result invalidates any chelation hypothesis and suggests that the detoxification process is rather based on the transport of cadmium. We thereafter investigated whether the complementation of Δ*ycf1* by AtHMA3 is related to a Cd release from the cells or rather due to an intracellular sequestration. Our previous results show that Δ*ycf1* complementation by AtHMA4 is correlated with a two-fold decrease in the intracellular Cd content. We concluded that the AtHMA4 phenotypic complementation of Δ*ycf1* is related to Cd release into the culture medium (submitted paper). In contrast, in the case of AtHMA3, ICP experiments showed that the Δ*ycf1* complementation is not correlated to an intracellular Cd decrease, suggesting that Cd is not expulsed from the cells but rather sequestered in a subcellular compartment. This hypothesis is supported by our observations with the confocal microscope. Although very low, the GFP fluorescence was always detected in the vacuole. The GFP fluorescence observed inside the vacuole could be due to intravacuolar proteasic activity resulting in the degradation of the fusion protein. It could be also due to aggregation of AtHMA3 proteins in clusters.

Our hypothesis of a vacuolar sequestration is consistent with the fact that AtHMA3 does not enhance Cd tolerance in a wild-type strain. Indeed, when simultaneously expressed, YCF1 and heterologous AtHMA3 could have redundant roles in yeast Cd detoxification. Expression of AtHMA3::GFP slightly enhances Cd tolerance but does not enhance Pb tolerance of Δ*ycf1*, suggesting that the C-terminal part of AtHMA3 could be involved in metal recognition and/or loading and that GFP perturbs this process.

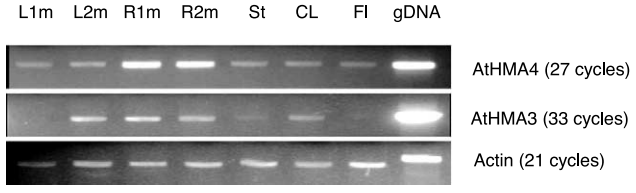

Fig. 5. AtHMA3 mRNA expression levels. Actin, AtHMA3 and AtHMA4 cDNA amplifications are detectable respectively after 21, 27 and 33 cycles. L1m/L2m: 1 or 2 months old rosette leaves; R1m/R2m: 1 or 2 months old roots; St, stem; CL, cauline leaves; Fl, flowers.

4.2. Speculations on HMA3 function in planta

The fact that AtHMA3 mRNA is detected at very low levels in tissues compared to AtHMA4, with a different tissular distribution, suggests that those transporters could have distinct roles in plant. Despite AtHMA3::GFP is addressed to the vacuolar membrane in the yeast context, this is not sufficient to exclude another location in *Arabidopsis*. The absence of a transit peptide suggests that AtHMA3 is not addressed to the chloroplast, as it is the case for PAA1, but probably rather to the tonoplast or plasma membrane.

In eukaryotes, P_{1B}-ATPases are most of the time involved in essential metal trafficking, allowing supply of metals such as Cu to metalloproteins in specific compartments (CCC2 in yeast [21], Menkes/Wilson ATPases in human [24] and PAA1 and RAN1 in *A. thaliana*). In contrast, in prokaryotes, P_{1B}-ATPases often play a role in cell detoxification, both for non-essential ions as Cd or Pb, and for excessive concentrations of essential metals such as Zn and Cu. Sequence alignments classify AtHMA3 in the Zn/Cd/Pb/Co P_{1B}-ATPases. However AtHMA3 failed in enhancing Zn tolerance of the wild-type yeast strain, and failed also in complementing the Zn-sensitive mutant Δ*zrc1*. Our results show that AtHMA3 is more efficient to transport Cd and Pb, suggesting a role in the transport of those toxic elements in *A. thaliana*. In that regard, the eukaryotic AtHMA3 could have a detoxification function, usually found in prokaryotes. Current work in our lab is aimed at verifying this hypothesis. This would be consistent with the hypothesis of a prokaryotic origin of AtHMA1–4 through horizontal transfer [25].

Acknowledgements: This work was supported by the Toxicologie Nucléaire program of the CEA. We thank Sandra Prévéral for the generous gift of the pYES2-GFP and pYES2-YCF1::GFP plasmids.

References

[1] Axelsen, K.B. and Palmgren, M.G. (1998) J. Mol. Evol. 46, 84–101.
[2] Moller, J.V., Juul, B. and Le Maire, M. (1996) Biochim. Biophys. Acta 1286, 1–51.
[3] Baxter, I., Tchieu, J., Sussman, M.R., Boutry, M., Palmgren, M.G., Gribskov, M., Harper, J.F. and Axelsen, K.R. (2003) Plant Physiol. 132, 618–628.
[4] Krämer, U. and Chardonnens, A.N. (2001) Appl. Microbiol. Biotechnol. 55, 661–672.
[5] Clemens, S. (2001) Int. J. Occup. Med. Environ. Health 14, 235–239.
[6] Song, W.-Y., Sohn, E.J., Martinoia, E., Lee, Y.J., Yang, Y.-Y., Jasinski, M., Forestier, C., Hwang, I. and Lee, Y. (2003) Nat. Biotechnol. 21, 914–919.
[7] Hirayama, T., Kieber, J.J., Hirayama, N., Kogan, M., Guzman, P., Nourizadeh, S., Alonso, J.M., Dailey, W.P., Dancis, A. and Ecker, J.R. (1999) Cell 97, 383–393.
[8] Woeste, K.E. and Kieber, J.J. (2000) Plant Cell 12, 443–455.
[9] Shikanai, T., Müller-Moulé, P., Munekage, Y., Niyogi, K.K. and Pilon, M. (2003) Plant Cell 15, 1333–1345.
[10] Axelsen, K.B. and Palmgren, M.G. (2001) Plant Physiol. 126, 696–706.
[11] Rosen, B.P. (2003) Comp. Biochem. Physiol. A Mol. Integr. Physiol. 133, 689–693.
[12] Rensing, C., Sun, Y., Mitra, B. and Rosen, B.P. (1998) J. Biol. Chem. 273, 32614–32617.
[13] Binet, M.R.B. and Poole, R.K. (2000) FEBS Lett. 473, 67–70.
[14] Liu, T., Nakashima, S., Hirose, K., Uemura, Y., Shibasaka, M., Katsuhara, M. and Kasamo, K. (2003) FEBS Lett. 542, 159–163.
[15] Mills, R.F., Krijer, G.C., Baccarini, P.J., Hall, J.L. and Williams, L.E. (2003) Plant J. 35, 164–176.
[16] Verwoerd, T.C., Dekker, B.M. and Hoekema, A. (1989) Nucleic Acids Res. 17, 2362.
[17] Gietz, D., St Jean, A., Woods, R.A. and Schielstl, R.H. (1992) Nucleic Acids Res. 20, 1425.
[18] Vida, T.A. and Emr, S.D. (1995) J. Cell Biol. 128, 779–792.
[19] Kwak, J.M., Murata, Y., Baizabal-Aguirre, V.M., Merril, J., Wang, M., Kemper, A., Hawke, S.D., Tallman, G. and Schroeder, J.T. (2001) Plant Physiol. 127, 473–485.
[20] Li, Z.S., Szczypka, M., Lu, Y.P., Thiele, D.J. and Rea, P.A. (1996) J. Biol. Chem. 271, 6509–6517.
[21] Yuan, D.S., Stearman, R., Dancis, A., Dunn, T., Beeler, T. and Klausner, R.D. (1995) Proc. Natl. Acad. Sci. USA 92, 2632–2636.
[22] Rad, M.R., Kirchrath, L. and Hollenberg, C.P. (1994) Yeast 10, 1217–1225.
[23] Shiraishi, E., Inouhe, M., Joho, M. and Tohoyama, H. (2000) Curr. Genet. 37, 79–86.
[24] Lutsenko, S. and Petris, M.J. (2002) J. Membr. Biol. 191, 1–12.
[25] Cobbett, C.S., Hussain, D. and Haydon, M.J. (2003) New Phytol. 159, 315–321.
[26] Williams, L.E., Pittman, J.K. and Hall, J.L. (2000) Biochim. Biophys. Acta 1465, 104–126.